Investigation of Correlation of Broadband UVA Reflection to Broadband Visible Reflection for a Variety of Surfaces in the Built Environment

Joanna Turner*[1], Alfio V Parisi[1]

[1]Faculty of Health, Engineering and Sciences, University of Southern Queensland, Toowoomba, QLD, Australia.

*Corresponding author (joanna.turner@usq.edu.au)

Summary of Declaration

Declaration of Interests: None

Abstract

UVA radiation (320-400 nm) exposure is linked to detrimental health effects, including DNA damage, eye damage and impacts on immune suppression. Occupational exposure to UVA radiation could increase the risk of developing such health effects, through increased exposure from reflective surfaces. A range of surfaces have been investigated for broadband (from spectral) UVA and visible reflectance, from horizontal, inclined and vertical orientations. A selection of this data has been presented graphically. Non-metallic and coated metallic surfaces were shown to have low UVA broadband reflectance (<0.20) compared to some metallic surfaces UVA broadband reflectance (0.1-0.5). Uncoated metallic surfaces can use UVA reflectance as a function of visible reflectance, however non-coated metallic surfaces have no similar function. The metallic surface type data were used to correlate UVA broadband reflectance to visible broadband reflectance and a model developed to express UVA broadband as a function of visible reflectance. The model for zinc aluminium coated steel is a linear regression, with UVA reflectance ranging from 0.09 to 0.46 and visible reflectance ranging from 0.05 to 0.57, with an R^2 of 0.95. The reflective coefficients used to create the model were produced on a solar zenith angle (SZA) range of 18°- 70.5°. The model was tested on a different dataset with a SZA range of 5.7°- 62.9° on clear days and was shown to have reasonable results with an RMSE of 0.049 for prediction of UVA reflectance from visible reflectance allowing prediction of the UVA reflectance from the visible reflectance for this surface type.

Keywords:

UVA radiation, visible radiation, reflectance, model, specular, zinc aluminium steel

1.0 Introduction

Quantification of solar radiation reflectance within the built environment is very important for a range of issues in the biosphere. Ultraviolet (UV) radiation reflectance contributes to increased risk of certain types of skin cancer [1-3] by increasing UV exposure to outdoor workers, while thermal and infrared radiation reflectance contributes to heat islands and energy balance issues at the building level through to urban canyons [4, 5]. Visible radiation reflectance is important due to potential distractions through glare, and there is an identifiable lack of regulation surrounding both visible reflection and thermal reflection, specifically due to uncontrolled reflections that could cause damage via human distraction or focused thermal reflection [6]. The biological impact of UV radiation on humans in the biosphere, correlated with quantification of UV reflectance is slowly increasing, however the ability to measure UV reflection is not always simple, given it mostly requires more specialised equipment. Research has been done previously to correlate calculation of UV irradiance incident at the earth's surface to the remaining terrestrial solar irradiance spectrum, by using ratios of separate components of visible spectra, and infrared and global solar terrestrial irradiance spectra [7, 8]. The authors propose that it should be possible that UV reflectance could be predicted from visible reflectance for some surface types. A study that characterises UV, visible and infrared reflectance has been carried out by Berdahl and Bretz [9], but only total solar reflectance and thermal emittance are correlated in this study. To the authors' knowledge, there is no research yet that seeks to combine information about proportionality between UV reflectance and visible reflectance directly in the built environment.

Research conducted prior to 1950, shows that reflectance from surfaces has been measured for metals used in daylighting or germicidal studies [10-17]. Research starting from 1925, but mostly from more recent decades, provides albedo measurement from natural and built surfaces measured in the broadband [18-25] or spectrally [26-31]. Reflectance of roofing materials have been documented, but only for horizontal orientations or else conducted in the lab [32, 33]. In the last decade, the authors have investigated reflectance from non-horizontal surfaces in the built environment (in the field) to compare to horizontal surfaces [34-38]. The reflectance from primarily vertical surfaces raised issues with terminology, such as the usage of reflectance versus albedo. The definition of albedo is defined as the fraction of incident sunlight that a surface reflects [39] however in many fields, the definition of albedo has been understood as the ratio of the *up-welling* reflected irradiance to *down-welling* incident irradiance, sometimes called the surface albedo (for remote sensing or similar fields) or hemispherical albedo (in planetary photometry). Hapke [40] provides several definitions for albedo and reflectance. The latter definition of albedo provided above does not entail a measurement that is appropriate for vertical surfaces. Turner and Parisi [34] show that using down-welling irradiance (all irradiance incident from a hemispherical range of 180°) created artificially inflated reflectance values due to the orientation of the surface (vertical) and the position of the sensor (with non-sun normal measurements). Reflectance ratios exceeded the maximum of 1.0 reflectance using the albedo definition of up-welling and down-welling irradiances, when measured in the field. In order to compare horizontal reflectance with vertical reflectance, measurements were made by taking incident irradiance from the direction of the sun with the sensor normal to the solar position. According to Hapke [41] this is called bidirectional reflectance and accounts for angle of incident irradiance. In past research conducted, most researchers have used down-welling measurements in their calculation of albedo. This paper will focus on the use of bidirectional reflectance, and will hereafter be referred to as reflectance for this study. Figure 1 (a) and (b) provide visual illustration of albedo and reflectance.

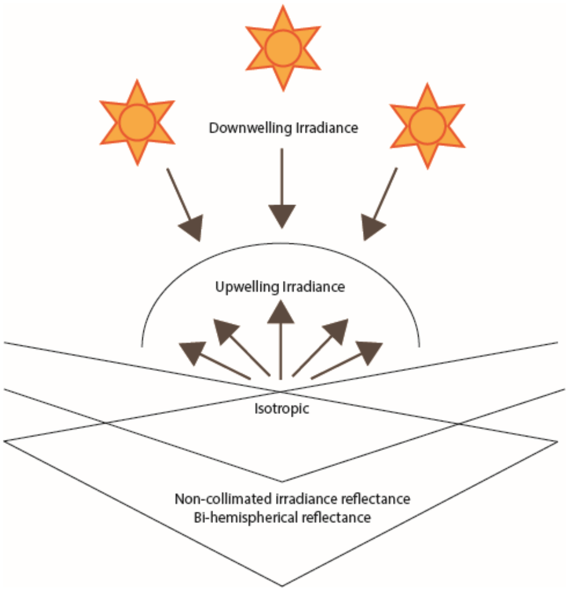

Figure 1- (a) albedo, as defined by the ratio of upwelling to downwelling irradiance. This can also be referred to as bi-hemispherical reflectance defined by Hapke [41]

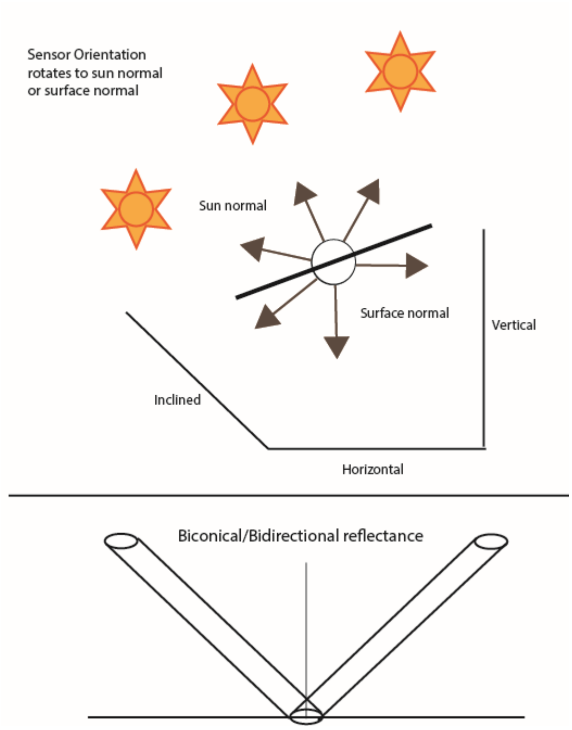

Figure 1 - (b) reflectance as defined by the ratio of the reflected irradiance to incident irradiance from a surface, which is dependent on angle of incidence and orientation of the surface (top image).The sensor is rotated to be normal to sun and surface. Hapke [41] similarly describes this as bidirectional reflectance, or biconical reflectance which implies a collimated beam of radiation (bottom image).

Reflectance and albedo are strongly dependent on the surface type, and measured reflectance will include different reflection characteristics of the surface, such as diffuse reflection (Lambertian reflection), specular reflection (Fresnel reflection) or more commonly, some combination of both diffuse and specular reflection. Coakley states that [39] it is assumed that surfaces reflect isotropically (evenly and in all directions) which thus means that the incident irradiance has no effect on the resultant reflectance and are therefore a Lambertian surface. Some natural surfaces can be assumed to be an approximate Lambertian surface, but many surfaces, both natural and built, tend to show variation of reflectance dependent on the incident irradiance angle. Previous work has already shown a number of building materials reflect anisotropically, and therefore indicates the surfaces are not predominantly Lambertian [34, 35]. In computer modelling studies of reflectance from surface, bidirectional reflectance is more pronounced on specular surfaces compared to diffuse surfaces with the difference described using clear spikes or lobes observed [42]. However Hapke [41] indicates that descriptors such as directional, conical or hemispherical are more appropriate in understanding reflectance which can describe both the incident and reflected radiation more accurately (hence “bi-directional” describes highly collimated radiation source and reflection). Research also shows that particle size of the surface controls the amount of specular or diffuse reflectance from a surface, with the larger the particle with respect to wavelength, the more diffuse the reflectance becomes [43]. Therefore the more smooth a material, the smaller the surface particles should be and hence more likely to produce specular reflection. Turner and Parisi’s [37] work on change in UV exposure due to surface reflectance suggests that variation in exposure to body site is due to the directional nature of reflectance from specific built surface types.

Very little work has been conducted on broadband UVA (320-400 nm) reflectance, where UVA reflectance measurement normally occur as part of a larger spectral measurement [26-30] or measured reflectance at a large distance from a surface [44, 45] rather than in close proximity (defined as within 1 metre of a surface for this study). UVA radiation comprises 6.3% of the total solar spectrum outside the earth's atmosphere [46] and undergoes much less attenuation compared to UVB radiation (280 nm-320 nm), making up to 95% of all terrestrial solar UV radiation [47]. Within the region of the solar spectrum, UVA radiation and visible radiation are the most similar and located consecutively within the same area of the solar spectrum. When this is combined with the reduced amount of attenuation of UVA in the atmosphere, it means the two areas of the spectrum will be the most likely to show comparable features and will hopefully provide an example for extension into future studies. Whilst UVA radiation is less biologically effective than UVB radiation at causing detrimental impacts (erythema and skin cancer), UVA radiation is also implicated in other health processes due to its ability to penetrate deeper into skin, eyes and other biological surfaces. Damage caused by UVA includes damage to DNA and the eye [48] and is potentially involved in the processes of immune suppression [47]. Occupational exposure is linked to increased risk of developing skin cancer [1, 3], therefore increased exposure to UVA reflectance could increase risk in all of the detrimental biological effects described. Increased UVA exposure due to reflective surfaces therefore needs to be explored and determining alternative methods to measure it may assist in reducing occupational UVA exposure. This research consists of two parts: (a) investigation of UVA broadband reflection from materials in the built environment that can influence occupational exposure and (b) investigation of the possibility of predicting UVA broadband reflection from broadband visible radiation reflection.

2.0 Methodology

Reflectance measurements were made using the techniques outlined in [34] which use sun normal measurements to replace down-welling irradiance measurements, and surface normal measurements to determine reflectance from horizontal and non-horizontal surfaces with the sensor located at 0.5 m from the surface (orientations as indicated in Figure 1 b) Measurements were made on a range of surfaces at the University of Southern Queensland, Toowoomba (27.5°S, 151.9°E). The main surface investigated was zinc aluminium coated steel with a trapezoidal profile, which is a commonly used building material in Australia. Aluminium [9], zinc and steel [11] are known reflectors of UV radiation. Most metal surfaces measured had a trapezoidal profile, while an additional similar surface type had a corrugated profile. The remaining surfaces were made up of trapezoidal profile steel sheeting with a coloured paint coating (multiple colours). Further surfaces investigated include red brick, white painted fibro board, galvanised steel and some non-structural based surfaces such as transparent plastic. An image of some of the surfaces is provided in Figure 2.

Figure 2 - Example of some surface types investigated.

The zinc aluminium and paint coated steel sheets were measured on horizontal, vertical and inclined (35° from the horizontal) orientations with all surfaces aligned to face towards the north, on clear days or partially cloudy days with the sun not obscured during measurement, and no shading on the reflective surface from the sensor. The remaining surfaces were measured from vertical, horizontal or inclined surfaces that were located in the local area depending on existing structures. For example, both the red brick and white painted fibro were only found in vertical orientations. The measurements were made between 2008 and 2012 with the data collected using a USB4000 Plug-and-Play Miniature fibre optic spectrometer (Ocean Optics, Inc.) from 300 nm to 700 nm in 0.2 nm steps, via an optic fibre and cosine corrector with a 180° field of view. The signal to noise ratio below 300 nm is poor, however given the solar terrestrial spectrum recorded at the earth's surface does not continue much lower than 300 nm due to absorption in the atmosphere and that this project focuses on the UVA radiation, this poses no issue to the data collected for this project. The USB4000 spectrometer has a 600 line blazed grating, a blaze wavelength of 400 nm and an opening slit of 25 µm. Each measurement is made with a data capture time of 20 ms and averaged from 20 scans. The USB4000 spectrometer was initially calibrated to a NIST traceable standard from 200 nm to 800 nm. UV measurements obtained using the USB4000 were then calibrated from 300 nm to 400 nm to a scanning spectroradiometer (model DTM 300; Bentham Instruments, Reading UK) located at the University of Southern Queensland (Toowoomba, Australia) which is traceable to the National

Physical Laboratory, UK. The measurements made by the calibrated USB4000 have an uncertainty of approximately ±10% across the UV spectrum and entire range of SZA. It is expected that visible measurements would have a minimum uncertainty of ±10%.

The data collected are spectral in nature, therefore the total broadband UVA reflectance and broadband visible reflectance, after calibration, were calculated by integrating across the ranges of 320 nm to 400 nm, and 400 nm to 700 nm respectively for UVA and visible radiation for each reflective surface and associated sun normal measurement, then calculating the reflectance by taking the ratio of the reflected broadband irradiance to the sun normal broadband irradiance as expressed in the following equation:

$$r = \frac{\int I_{r\lambda}\, d\lambda}{\int I_{i\lambda}\, d\lambda}$$

Where r is the broadband reflectance, $I_{i\lambda}$ is the sun normal irradiance, and $I_{r\lambda}$ is the reflected irradiance from the surface measured.

Reflected measurements were taken in succession after the sun normal measurements, with less than a minute between each measurement. Therefore the reflected irradiance measurements occur within one degree of SZA of the incident irradiance measurement. As the instrument records both UV and visible irradiance in the same measurement, matching UVA to visible reflection for SZA is straightforward. Data for each surface type and orientation were compiled for review. After reviewing the data, surface types were selected to determine if visible broadband reflection could be used to predict UVA broadband reflection. The selected surface type was zinc aluminium trapezoidal due to there being a suitable spread of data available for this surface type, across different orientations, as well as the results found from the initial survey of data. From previous research, it is also suspected that the surface is dominated by specular reflection, despite not appearing to be a specular surface (mirror like) [43]. It is possible that a surface can still behave like a specular reflector in a non-visible spectrum despite not appearing to be “mirror” like to the eye.

Data collected from 2008 to 2010 was used to generate the model to predict UVA reflection from visible reflection and data collected from 2011 to 2012 were used to test the fit of the model. Residuals and root mean square error (RMSE) were calculated to determine best fit, along with the relative RMSE (rRMSE) which is defined as the ratio of the RMSE to the mean of the model result. It is also useful here to comment regarding reflectance measurement within the UVB spectrum. The equipment is capable of providing reflectance within the UVB spectrum down to 300nm without significant signal-to-noise issues, however, at these wavelengths, the total irradiance reaching the earth’s surface is small while showing correspondingly high reflectance. Spectral reflectance has been previously shown to be relatively high [36] at wavelengths below 320nm. However, the focus within this article is on the UVA and visible spectra, and therefore the data from 300nm to 320 nm is not provided here.

3.0 Results

Figure 3 shows the comparison of UVA reflectance to visible reflectance for zinc aluminium trapezoidal (n=398) and zinc aluminium corrugated surface types (n = 87). There is not enough zinc aluminium corrugated data to test for an appropriate statistical comparison, however Figure 3 shows that when producing a scatter plot of UVA broadband reflectance with respect to visible broadband reflectance, there is definitely a strong similarity in the characterisation of the surface types. It appears that the profile of the surface does not significantly change the reflectance characteristics provided the surface is made of the same material. Turner [49] has further data analysis from spectral analysis which confirms lack of significant difference between reflectance for profile types.

Figure 4 presents the data collected for metal surfaces only (n = 772). Three surface types have been previously investigated for influence to human exposure (zinc aluminium steel, pale green coated steel and cream coated steel) [37, 49], and have been plotted separately to the remaining types since there is significantly more data available in these surface types compared to dark coloured paint coated steel and light coloured paint coated steel. The dark coloured paint coated steel includes black, blue, red and green – the latter colours all in dark shades. The light coloured paint coated steel consists of beige and a product coating called Insultec 4 (Insultec, Australia), which is a white coloured thermal radiation reflecting paint.

Figure 5 presents data collected from surfaces in the built environment from existing structures. The data collected from the red brick surface and the white painted fibro surface are for vertical structures with no inclined or horizontal features made out of the same surface material. The grey coated steel was located on the rooftop of a building at the University as a roofing surface. The thick transparent acrylic was also located on the roof. The grey paint coated steel was in a horizontal orientation only, while the thick transparent acrylic was featured in a skylight on the roof, with an inclination of approximately 45° to the horizontal. The galvanised steel (galvanised is normally understood to be a coating predominantly made with zinc) was very shiny to look at and therefore highly reflective in the visible spectrum, and was inclined at a small angle to the horizontal. The galvanised steel was part of a structure located on the top of the building near the skylight and roof surface.

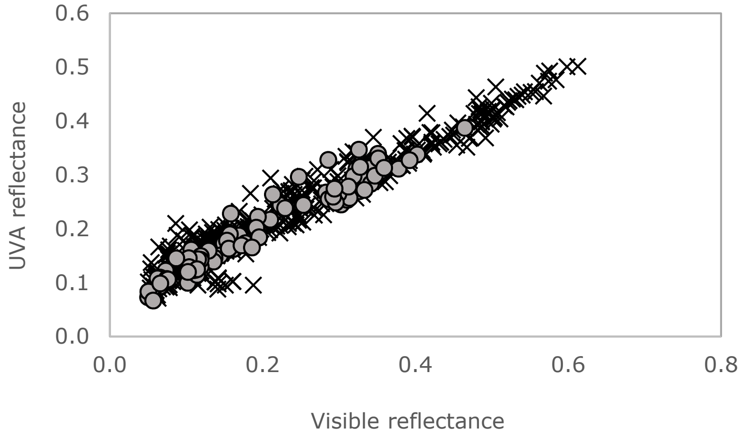

Figure 3 - Plot of UVA broadband reflectance with respect to visible broadband reflectance for zinc aluminium trapezoidal (x) surface (all orientations) and zinc aluminium corrugated (o) for all surface orientations.

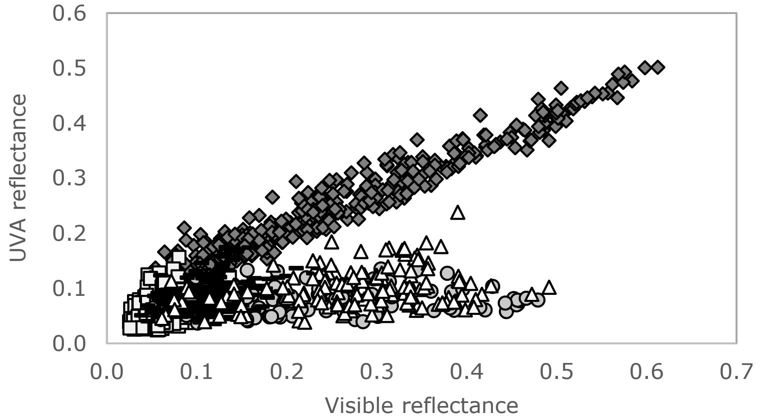

Figure 4 - UVA broadband reflectance with respect to visible broadband reflectance for metal surfaces of all profile types (trapezoidal and corrugated) for dark colour paint coated (square ☐), light coloured paint coated (circle ○), zinc aluminium (diamond◆), cream paint coated (triangle Δ) and pale green paint coated (-).

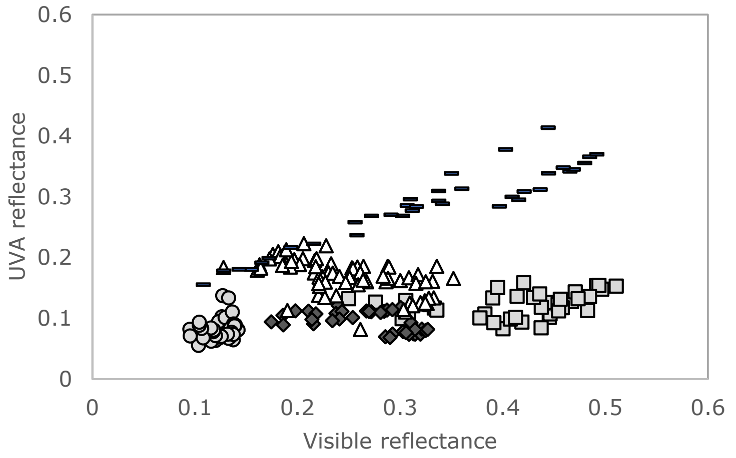

Figure 5 - UVA broadband reflectance with respect to visible broadband reflectance for white painted fibro board (square ☐), red brick (circle ○), grey paint coated steel (diamond◆), thick transparent acrylic (triangle Δ) and galvanised steel (dash -).

Figures 6 (a) and 6 (b) demonstrate the spectral reflectance of a variety of the surface types investigated, for reflectance that has been measured at about 50° SZA and 30°SZA. Figure 6 (c) shows reflectance measured at approximately 65-70° SZA and 50° SZA as the data was collected on days with a low SZA range.

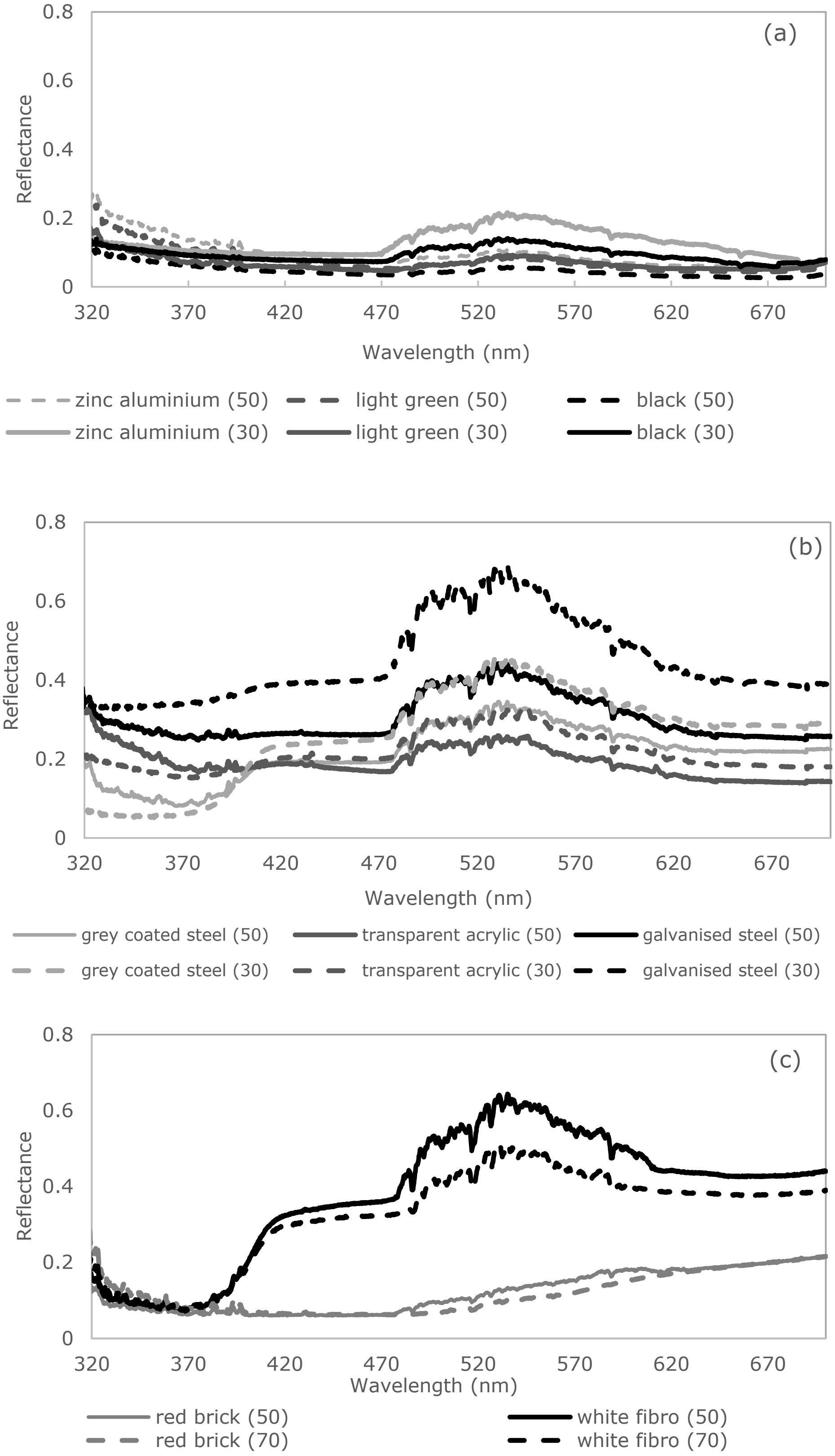

Figure 6 - (a) Spectral reflectance for vertical trapezoidal surfaces at two different solar zenith angles (b & c) Spectral reflectance from local building materials in existing structures at the different SZA shown in brackets

Figure 6 provides spectral information about the behaviour of reflectance from a surface with respect to SZA. From the figure it can be observed that for the surfaces in Figure 6a, the UVA reflectance over the waveband decreases when SZA decreases, whereas the visible reflectance over the waveband increases. In Figure 6b, grey coated steel and transparent acrylic decrease UVA spectral reflectance with SZA, whereas the visible spectral reflectance increases. However, galvanised steel increases with decreased SZA for both UVA spectral reflectance and visible spectral reflectance. Figure 6c shows that UVA spectral reflectance does not vary significantly during a decrease in SZA, whereas the visible spectral reflectance does increase for white painted fibro. Red brick appears to remain the same for the UVA spectral reflectance and most of the visible spectral reflectance.

From this presented information, a general assessment can be made about what mechanism might be contributing to the relationships presented in Figures 4 and 5 for broadband reflectance in the UVA and visible spectra. In Figure 4, zinc aluminium steel shows that as UVA broadband reflectance increases overall, so too does visible broadband reflectance. We can also observe in Figure 6a, that the UVA spectrum shows higher reflectance in the shorter UVA wavelengths at higher SZA than the longer UVA wavelengths, but with an increase in SZA, the UVA reflectance becomes more consistent across the spectrum. As there is more prevalence of longer UVA wavelengths in the atmosphere compared to shorter UVA wavelengths, the incident irradiance on the measured surface thus accounts for the change in proportion of longer to shorter UVA wavelengths. For the paint coated steel surfaces, we can see that the UVA broadband reflectance does not increase with visible broadband reflectance in Figure 4. This could be due to the nature of the paint coating, however it is interesting that the black coated surface shows an increase in visible spectral reflectance. The black paint coated surface appears shiny when in use from certain angles of view, more so than the pale green coated surface. This could suggest that the black paint coating may consist of smaller particles or a reduced layer of particles on the coated steel. However, as black is a good absorber of thermal energy and is not always desirable for use in common building practice, the reflectance properties within the visible or the UVA spectra are unlikely to be as useful or practical compared to the more commonly used surface types. In Figure 5, galvanised steel shows a similar relationship between UVA broadband reflectance and visible broadband reflectance as compared to zinc aluminium steel. It is also notable that the surfaces that have already been previously identified as more specular reflecting surfaces than the paint coated surfaces, show a potential linear regression relationship between UVA broadband reflectance and visible broadband reflectance. On consideration of the spectral nature of the reflectance of the galvanised and zinc aluminium steel surfaces, we can observe that the spectral reflectance tends towards a more consistent or even reflectance across both spectra. This then suggests that predominantly specular reflecting surfaces are more likely to have a predictive relationship between the UVA reflectance and the visible broadband reflectance. Therefore, the zinc aluminium steel surface has been used to investigate a model to predict UVA broadband reflectance.

3.1 Predictive model for zinc aluminium surfaces

The following section focuses on data collected for the zinc aluminium trapezoidal sheet surface. The data from 2008 to 2010 were collected in May 2008, October 2008, April 2009, August and October 2010 with a total of 209 measurements made from vertical, inclined and horizontal surface measurements with a SZA range from 14.0° to 70.5°. Figure 7 shows the data according to surface orientation (vertical, horizontal and inclined) and displays for all data included in this set, with the regression line of best fit $y = 0.7242x + 0.0695$ and $R^2 = 0.91$. Here, y is the UVA broadband reflectance and x is the visible broadband reflectance. The broadband reflectance ranges are 0.09 - 0.46 for UVA reflectance and 0.05 - 0.57 for visible reflectance.

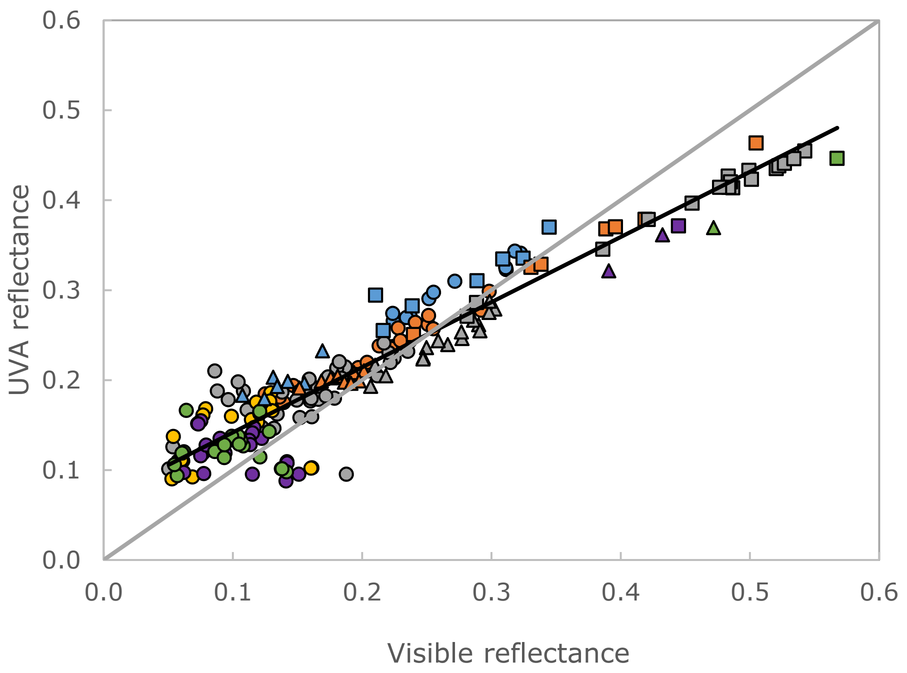

Figure 7 – Broadband UVA reflection to visible reflection, for each surface orientation of vertical (circles ○), horizontal (triangles Δ) and inclined (squares □). SZA ranges are >60 (blue), 50-59.9 (orange), 40-49.9 (grey), 30-39.9 (yellow), 20-29.9 (purple) and <20 (green). Trend line of all data (black unbroken line) and one to one line (grey unbroken line).

In Figure 7, there is data that does not fit the regression line particularly well. This data is from October 2008 from a vertical surface only, and shows an unusual spread that appears to oppose the general trend of the data. It appear to look more like data presented in Figure 5 for the red brick. The data of poor fit is mostly found to have a SZA of less than 20° with one or two outliers in 30-39.9° and 40-49.9 It was considered whether the smaller SZA, might contribute to an incident angle that behaves more like a grazing angle. A grazing angle is either a very large or very small incident angle, depending on whether it is measured from the horizontal or the normal of the surface. Grazing angle reflectance can produce very high reflectance coefficients. However, these broadband reflectance values are fairly low. The other possibility is that given the directional nature of the reflectance measurement, the sensor may not capture the total reflected irradiance at these incident angles. A preview of the 2011 and 2012 data shows that SZA smaller than 20° do not show the same poor fit to a regression line as the data shown in Figure 7. Therefore the October 2008 data were removed in case of other confounding errors that are not yet apparent. The removal of the data adjusted the line of regression to $y = 0.7239x + 0.0718$ with a correlation of $R^2 = 0.95$. The refined data is shown in Figure 8 with respect to surface orientation. The total SZA range is not affected by removing this data, with a range of 18°-70.5° with a total of 171 data values. Figure 9 shows the SZA spread associated with the data for both the original data set (Figure 7) and the refined data set (Figure 9). The range of reflection coefficients remains unchanged, with UVA reflection coefficients of 0.09 - 0.46 and visible reflection coefficients of 0.05 - 0.57.

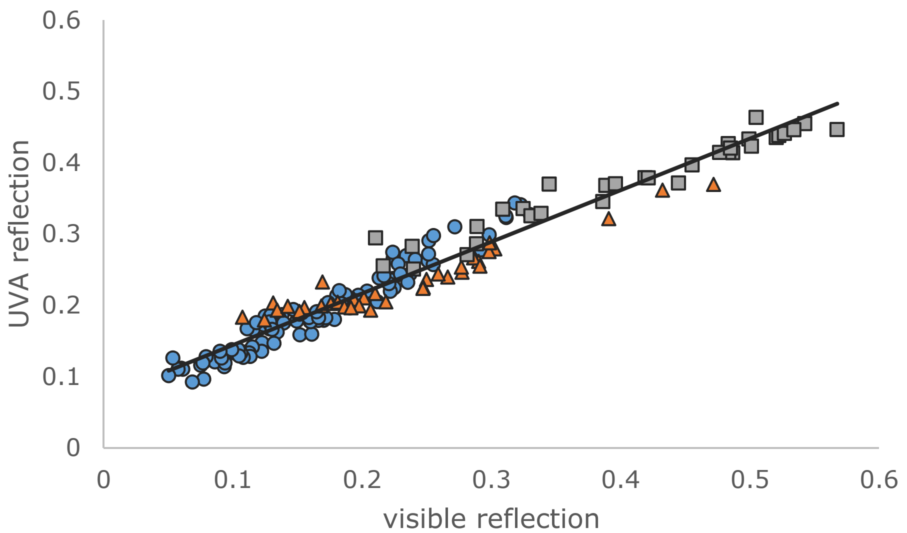

Figure 8 - Refined data with regression model of data. UVA reflection to visible reflection matched for SZA, for each surface orientation of vertical (circles), horizontal (triangles) and inclined (squares).

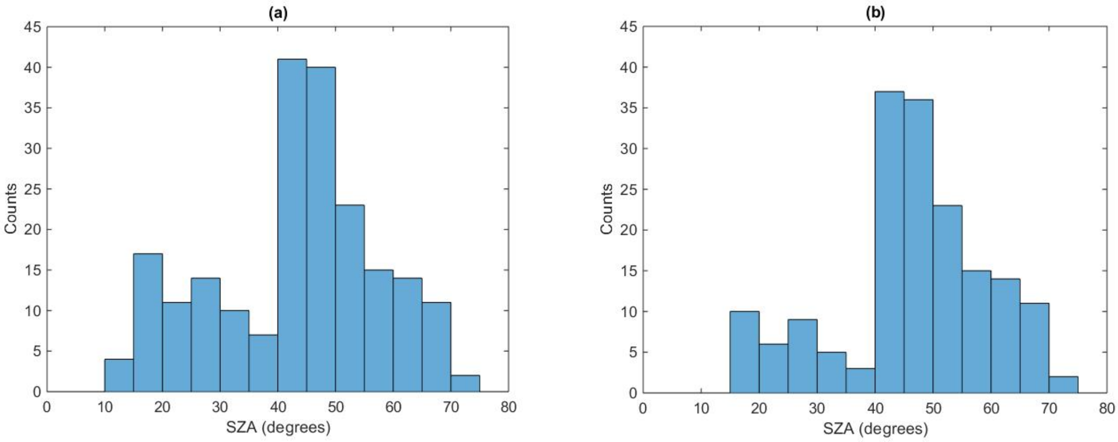

Figure 9 – (a) Histogram of SZA range for 209 data values used to create model (minimum of 14° and maximum of 70.5°) (b) Histogram of SZA range for 171 data values used to create model (minimum of 18° and maximum of 70.5°).

Each of the regression models presented here were tested and validated using data collected in September 2011 and January 2012 that had a total of 178 data values, with a SZA range of 5.7° to 62.9°. The residuals of each regression model were reviewed. Initially the RMSE of the refined data were shown to be greater than using a model with the included October 2008 data, which was surprising. However, on closer inspection of the residuals for each version of the model, it was found that there was some bias in both models by means of overestimating UVA broadband reflectance from visible broadband reflectance. Using the residuals as a guide to adjust each model, it was found that the best model to predict data were $y = 0.7239x + 0.0518$ which is created from the model that did not include the October 2008 data. The RMSE for this model was calculated as 0.049. The calculated RMSE and rRMSE's for each model type is provided in Table 1. Figure 10 shows the data used to validate the model and the refined model, while Figure 11 provides information about the residuals from the model.

Table 1 - RMSE, rRMSE for models devised to predict UVA reflection from visible reflection.

Model	RMSE	rRMSE
All data $y = 0.7242x + 0.0695$	0.188	0.69
Refined data $y = 0.7239x + 0.0718$	0.217	0.54
All data revised $y = 0.7242x + 0.0595$	0.054	0.21
Refined data revised $y = 0.7239x + 0.0518$	0.049	0.19

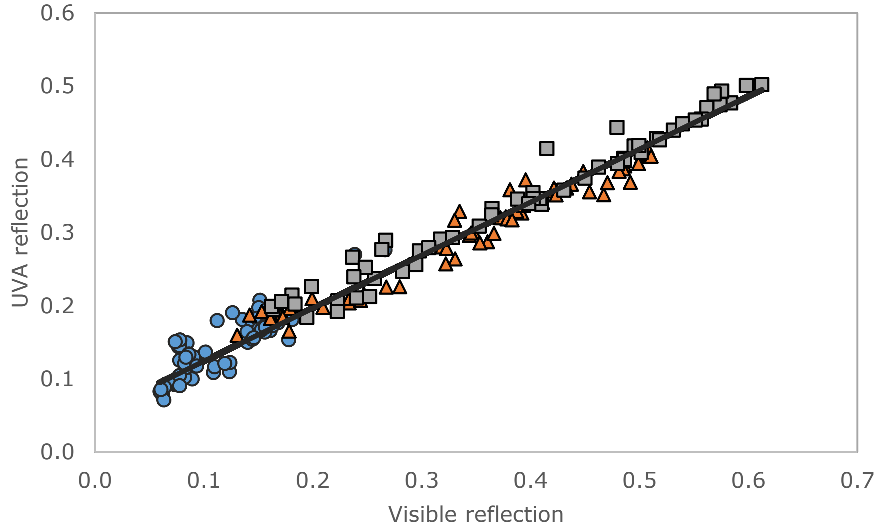

Figure 10 - Validation data from 2011 and 2012 for surface orientation of vertical (circles), horizontal (triangles) and inclined (squares) and associated predicted values from refined model (line) for zinc aluminium surfaces.

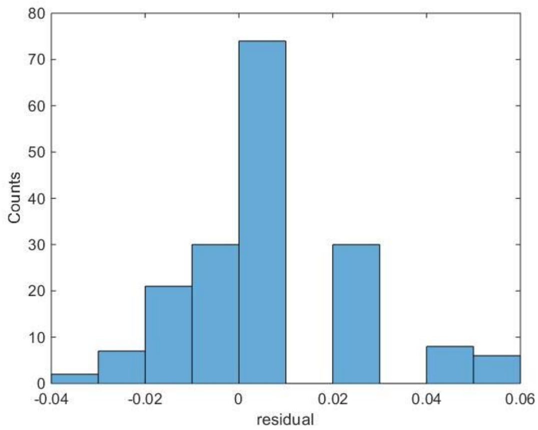

Figure 11 - Histogram of residuals for the model used to predict UVA reflection from visible reflection.

4.0 Discussion

The results show that zinc aluminium coated steel with a trapezoidal profile has a UVA broadband reflectance which can be estimated using a simple regression model based on visible broadband reflectance. In general, we can make a statement regarding UVA broadband reflectance from built materials with respect to visible broadband reflectance. Non-metallic surfaces and paint coated metallic surfaces do not show UVA broadband reflectance as a function of visible broadband reflectance. The reflectance values are in general 0.2 or below. While this will still contribute to UVA exposure on a nearby person, it is currently unknown if this reflectance value would cause a significant increase to the overall UV exposure received. However, for individuals that work near metallic shiny surfaces, if visible reflectance is high, UVA reflectance will also be high. In turn this contributes to an increase in UVA exposure. The ability to predict UVA broadband reflectance from visible reflectance means that outdoor workers are able to better assess their surrounding work area for increased UVA hazards. The limitations to this model are that it is only appropriate for clear sky days or when the sun is not obscured on partially cloudy days, and is only relevant to uncoated metallic surfaces. If the sun is obscured, the reflectance is affected by the reduction of direct irradiance on the reflective surface. This is already evident by the different spectral reflectance for changing SZA. However, it appears that for different SZA ranges (Figures 7, 8 and 9), that large broadband reflectance do not always depend on large SZA and vice versa. This is particularly relevant for the vertical surface where SZA can be used as an approximate incident angle. To investigate this further, the ratio of the UVA reflection to the visible reflection was plotted against SZA (Figure 12) for zinc aluminium surface types (Figure 12a) and additionally a paint coated steel surface (Figure 12b).

Figure 12a shows that for zinc aluminium steel, the horizontal and inclined surface reflectance show a slight trend in the proportion of UVA broadband reflectance to visible broadband reflectance increasing at SZA of 40° or higher. The galvanised steel was also included in Figure 12a, and it also shows this slight trend. For vertical surfaces (zinc aluminium steel surfaces) however, there is no trend displayed. This may be due to the change in spectral reflectance over the day depending on the surface type. Figure 13 provides two different SZA scans for three surface orientations of zinc aluminium trapezoidal steel. For horizontal or inclined surface orientations, the UVA reflectance remains the same or increases with decreasing SZA, as does the visible reflectance.

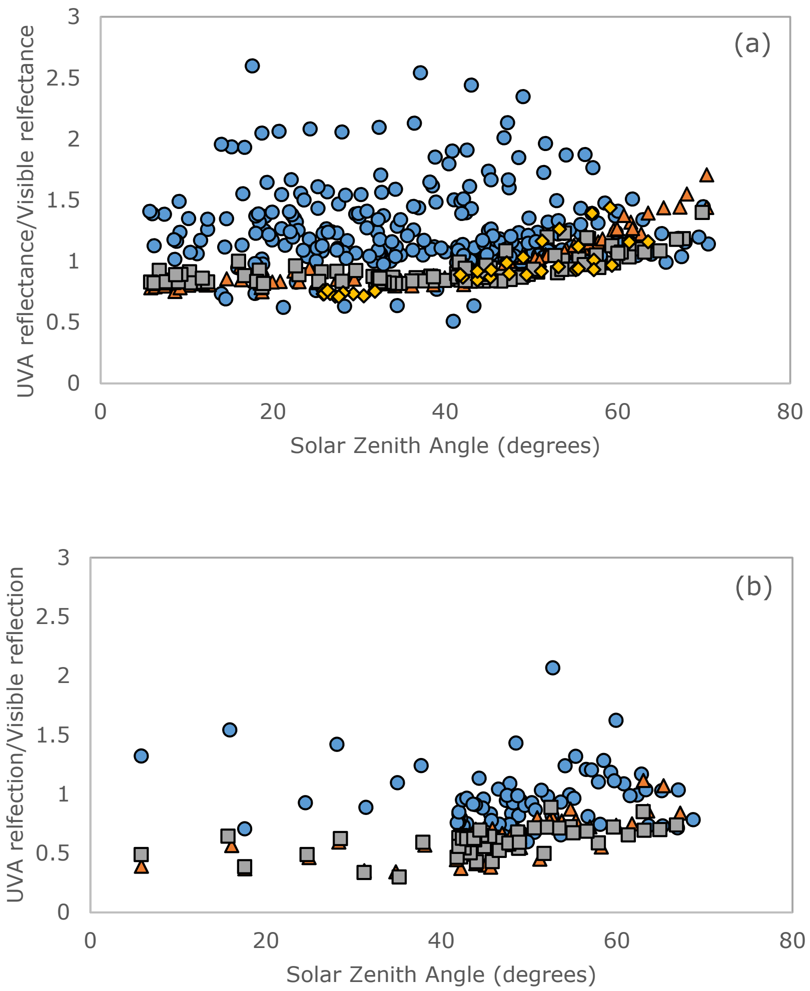

Figure 12 – Ratio of UVA reflection to visible reflection with respect to SZA for (a) vertical (circles), horizontal (triangles) and inclined (squares) surfaces for a zinc aluminium steel trapezoidal and corrugated surfaces and for a gentle inclined galvanised steel surface (diamonds) and (b) pale green coated trapezoidal surface.

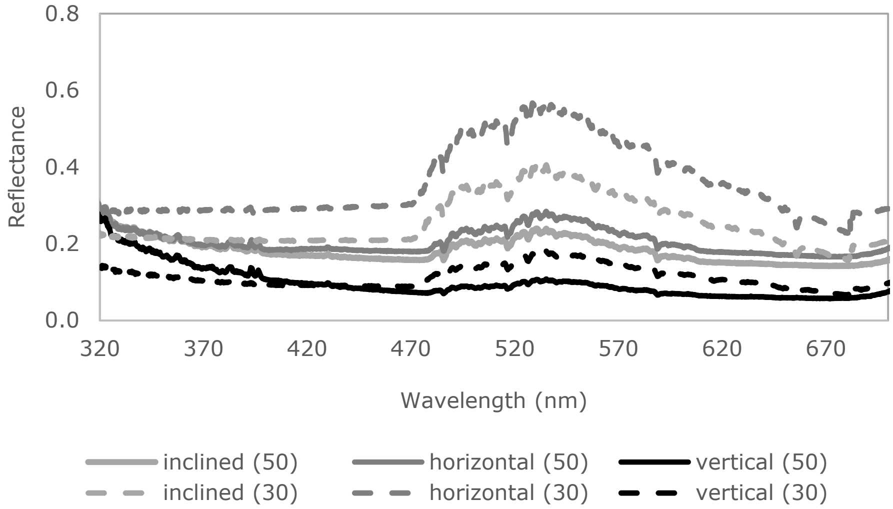

Figure 13 - Spectral reflectance from zinc aluminium trapezoidal steel for two different SZA for inclined, horizontal and vertical orientations.

However, the UVA reflectance from the vertical surface is lower at the lower SZA while the corresponding visible reflectance is higher. It is possible this inverse relationship between reflectance for this particular vertical surface provides some explanation for lack of predictable relationship between broadband UVA irradiance and broadband visible reflectance with respect to SZA shown in Figure 12 (a). Despite this identified lack of relationship in Figure 12, Figure 7, 8 and 9 clearly show that the broadband reflectance measured for UVA can be reasonably predicted from visible broadband reflectance for vertical surfaces. Figure 12(b) was included to determine if paint coated surfaces similarly show this effect, and Figure 14 displays the spectral reflectance for the same surface type (pale green coated trapezoidal) for each orientation at different SZA.

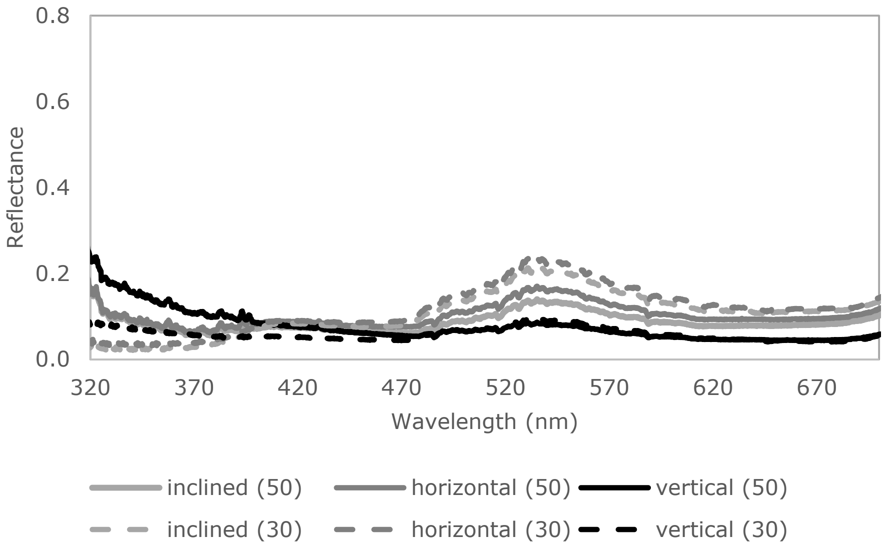

Figure 14 - Spectral reflectance from pale green paint coated trapezoidal steel for two different SZA for inclined, horizontal and vertical orientations.

UVA reflectance in Figure 14 is lower at lower SZA, while the corresponding visible reflectance is higher, except for the case of the vertical surface, which shows similar visible spectral reflectance for both SZA. If vertical surfaces do not show a change in visible reflectance with SZA, then it may not be possible to predict changes in UVA reflectance. However, reflectance from paint coated surfaces tends to be much lower than zinc aluminium surfaces, and appear to have low influence on human exposure [37, 38]. Therefore a predictive method of measuring UVA reflectance may not be necessary for the paint coated surface types given their low influence on increasing UV exposure. Comparison of non-painted metal surfaces to natural surfaces show a significant difference in reflectance. Figure 15 shows the difference between reflectance of a natural surface (lawn or grass) as measured by Feister and Grewe [26] compared to (not painted) zinc aluminium coated steel from this study. Non painted metal surfaces have been shown to increase UV exposure [37, 38]. Therefore, prediction of UVA reflectance from visible reflectance from non-painted surfaces with respect to low reflectance from common natural surfaces may be useful for determining changes to UVA exposure.

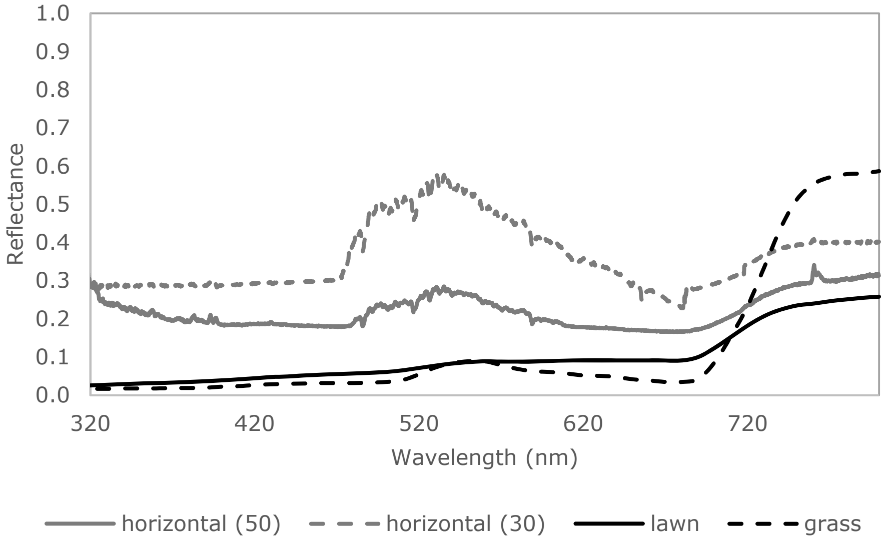

Figure 15 - Spectral reflectance from horizontal zinc aluminium coated steel at two different SZA and spectral reflectance from lawn and grass as measured by Feister and Grewe [26].

In terms of practical application for occupational workers, from the information presented in this research, measurement devices such as a simple lux meter or light meter could be used to measure the visible broadband reflectance of building materials, from which an estimation of the UVA reflectance for zinc aluminium surfaces could be determined. Steps could then be taken to ensure adequate personal protection is being used to prevent over exposure to UVA radiation.

Alternative opportunities for measuring visible reflectance can come from commonly used technology. Many smartphones now have applications that can provide light measurements and may also provide a method to estimate UVA reflectivity using the method developed in this research. Additionally recent work with smartphones [50, 51] have been shown to be capable of measuring UVA directly, which suggests the model in this paper may be able to be tested using different equipment (such as smartphones) in the future. Smartphone types that have not been characterised by the method used by Igoe et al., [51, 52] could be used to calculate UVA reflectance from visible reflectivity coefficients using the model presented here. Furthermore, a smartphone application could be developed that uses a smartphone's internal sensors to measure UVA reflectivity, from the visible reflection captured by the camera in the smartphone.

There is a number of future directions from which this work can progress, including determining if there is a relationship between biologically weighted UVA and visible radiation, or determining if there is a relationship between visible and UVB radiation reflectance. It is also important to investigate other surface types, both man-made and natural, for any possible associated relationships between UVA and visible reflection, particularly in the case of high coefficient reflecting surfaces. The most highly desirable future direction would be to explore the relationship between biologically weighted UV reflectance and biologically weighted visible weighted reflectance. For example, the erythemal weighted UV reflectance could be compared to photopic weighted visible reflectance (sensitivity of the human eye).

5.0 Conclusions

UVA radiation is associated with a number of biologically detrimental effects, and outdoor workers are exposed to these effects when they are involved in outdoor occupational activities. Occupational workers that need to work in areas of built materials that have high reflectivity in the UVA spectrum, increase their risk of developing health concerns due to exposure to UVA radiation. This paper has presented UVA and visible reflectance for a range of common building materials used in Australia. Spectral and broadband reflectance was presented for the range of surface types. It was found that non-metallic and some painted coated metallic surfaces had UVA broadband reflectance of less than 0.2 and will contribute to normal UV exposure through scattering from nearby surfaces. In contrast, metallic surfaces without a coating could have relatively high UVA broadband reflectance, which can be determined as a function of unweighted visible broadband reflectance and could potentially increase a person's UVA exposure significantly. The surface types that fit this model are steel coated in aluminium and zinc, or just zinc. The model developed has an R^2 of 0.95 and an RMSE of 0.049. Since the reflective surface shows that reflectance can change with respect to SZA, a model can assist the prediction of UVA reflectance to assist in determining personal protection.

6.0 Acknowledgements

The authors would like to thank the University of Southern Queensland for supporting this research.

7.0 References

1. Gies, H.P. and J. Wright, *Measured solar ultraviolet radiation exposures of outdoor workers in Queensland in the building and construction industry.* Photochemistry and Photobiology, 2003. **78**(4): p. 342-348.
2. Håkansson, N., et al., *Occupational sunlight exposure and cancer incidence among Swedish construction workers.* Epidemiology, 2001. **12**(5): p. 552-557.
3. Milon, A., et al., *Effective exposure to solar UV in building workers: influence of local and individual factors.* Journal of Exposure Science and Environmental Epidemiology, 2007. **17**: p. 58-68.
4. Arnfield, A.J., *Review: Two decades of urban climate research: a review of turbulence, exchanges of energy and water, and the urban heat island.* International Journal of Climatology, 2003. **23**: p. 1-26.
5. Fortuniak, K., *Numerical estimation of the effective albedo of an urban canyon.* Theoretical and Applied Climatology, 2008. **91**(1-4): p. 245-258.
6. Danks, R., J. Good, and R. Sinclair, *Assessing reflected sunlight from building facades: A literature review and proposed criteria.* Building and Environment, 2016. **103**: p. 193-202.
7. Escobedo, J., et al., *Modeling hourly and daily fractions of UV, PAR, and NIR to global solar radiation under various sky conditions at Botucatu, Brazil.* Applied Energy, 2009. **86**: p. 299-309.
8. Escobedo, J., et al., *Ratios of UV, PAR and NIR components to global solar radiation measured at Botucatu site in Brazil.* Renewable Energy, 2011. **36**: p. 169-178.
9. Berdahl, P. and S.E. Bretz, *Preliminary survey of the solar reflectance of cool roofing materials.* Energy and Buildings, 1997. **25**: p. 149-158.
10. Edwards, J.D., *Aluminium reflectors.* Transactions of the Illuminating Engineering Society, 1939. **34**: p. 427-440.
11. Hulburt, E.O., *The reflecting power of metals in the ultraviolet region of the spectrum.* Astrophysical Journal, 1915. **42**(3): p. 205-230.
12. Luckiesh, M., *Reflection and Transmission*, in *Applications of Germicidal, Erythemal and Infrared Energy*. 1946, D. Van Nostrand Company, Inc.: New York. p. 375-451.
13. Stutz, G.F.A., *Observations of spectro-photometric measurements of paint vehicles and pigments in the ultra-violet.* Journal of the Franklin Institute, 1925. **200**(1): p. 87-102.
14. Taylor, A.H., *Reflection factors of various materials for visible and ultraviolet radiation.* Journal of the Optical Society of America, 1934. **24**(7): p. 192-193.
15. Taylor, A.H., *Light and ultraviolet reflection by various materials.* Transactions of the Illuminating Engineering Society, 1935. **30**: p. 563-566.
16. Taylor, A.H., *Ultraviolet reflectance characteristics of various materials.* Illuminating Engineering, 1941. **36**: p. 927-930.
17. Wilcock, D.F. and W. Soller, *Paints to reflect ultraviolet light.* Industrial and Engineering Chemistry, 1940. **32**(11): p. 1446-1451.
18. Angstrom, A., *The albedo of various surfaces of ground.* Geografiska Annaler, 1925. **7**: p. 323-342.
19. Diffey, B., et al., *A portable instrument for measuring ground reflectance in the ultraviolet.* Photochemistry and Photobiology, 1995. **61**(1): p. 68-70.
20. Heisler, G.M. and R.H. Grant, *Ultraviolet radiation in urban ecosystems with consideration of effects on human health.* Urban Ecosystems, 2000. **4**: p. 193-229.

21. ICNIRP, *Protecting workers from ultraviolet radiation*. 2007, International Commision on Non-Ionising Radiation Protection.
22. Parisi, A.V., et al., *Lifetime ultraviolet exposure estimates for selected population groups in south-east Queensland.* Physics in Medicine and Biology, 1999. **44**: p. 2947-2953.
23. Reuder, J., et al., *Investigations on the effect of high surface albedo on erythemally effective UV irradiance: Results of a campaign at the Salar de Uyuni, Bolivia.* Journal of Photochemistry and Photobiology B: Biology, 2007. **87**: p. 1-8.
24. Rosenthal, F.S., et al., *The occular dose of ultraviolet radiation to outdoor workers.* Investigative Ophthalmology and Visual Science, 1988. **29**(4): p. 649-656.
25. Sliney, D.H., *Physical Factors in Cataractogenesis: ambient ultraviolet radiation and temperature.* Investigative Ophthalmology and Visual Science, 1986. **27**(5): p. 781-790.
26. Feister, U. and R. Grewe, *Spectral albedo measurements in the UV and visible region over different types of surfaces.* Photochemistry and Photobiology, 1995. **62**(4): p. 736-744.
27. Lester, R.A. and A.V. Parisi, *Spectral ultraviolet albedo of roofing surfaces and human facial exposure.* International Journal of Environmental Health Research, 2002. **12**: p. 75-81.
28. Lin, C., C. Han, and C. Liu, *A comparison of the albedo of Asian Building materials in visible and UVB regions*, in *International Conference on Electric Technology and Civil Engineering (ICETCE)*. 2011, IEEE: Lushan, China.
29. McKenzie, R.L., M. Kotkamp, and W. Ireland, *Upwelling UV spectral irradiances and surface albedo measurements at Lauder, New Zealand.* Geophysical Research Letters, 1996. **23**(14): p. 1757-1760.
30. Webb, A., et al., *Airborne spectral measurements of surface reflectivity at ultraviolet and visible wavelengths.* Journal of Geophysical Research, 2000. **105**(D4): p. 4945-4948.
31. Coulson, K.L. and D.W. Reynolds, *The spectral reflectance of natural surfaces.* Journal of Applied Meteorology, 1971. **10**(6): p. 1285-1295.
32. Kültür, S. and N. Türkeri, *Assessment of long term solar reflectance performance of roof coverings measured in laboratory and in field.* Building and Environment, 2012. **48**: p. 164-172.
33. Parker, D.S., et al. *Laboratory testing of the reflectance properties of roofing materials*. Florida Solar Energy Center, 2000.
34. Turner, J. and A. Parisi, *Improved method of ultraviolet radiation reflection measurement for non-horizontal urban surfaces.* Measurement Science & Technology, 2012. **23**(4).
35. Turner, J. and A. Parisi, *Ultraviolet Reflection Irradiances and Exposures in The Constructed Environment For Horizontal, Vertical and Inclined Surfaces.* Photochemistry and Photobiology, 2013. **89**(3): p. 730-736.
36. Turner, J., A. Parisi, and D. Turnbull, *Reflected solar radiation from horizontal, vertical and inclined surfaces: Ultraviolet and visible spectral and broadband behaviour due to solar zenith angle, orientation and surface type.* Journal of Photochemistry and Photobiology B-Biology, 2008. **92**(1): p. 29-37.
37. Turner, J. and A.V. Parisi, *Measuring the influence of UV reflection from vertical metal surfaces on humans.* Photochemical & Photobiological Sciences, 2009. **8**(1): p. 62-69.
38. Turner, J. and A.V. Parisi, *Influence of reflected UV irradiance on occupational exposure from combinations of reflective wall surfaces.* Photochemical & Photobiological Sciences, 2013. **12**(9): p. 1589-1595.
39. Coakley, J.A., *Surface Reflectance and Albedo*, in *Encyclopedia of Atmospheric Sciences*, R.H. James, Editor. 2003, Academic Press: Oxford. p. 1914-1923.
40. Hapke, B., *Integrated reflectances and planetary photometry*, in *Theory of reflectance and emittance spectroscopy*. 2012, Cambridge University Press: Cambridge, United Kingdom. p. 287-302.
41. Hapke, B., *The bidirectional reflectance of a semi-infinite medium*, in *Theory of Reflectance and Emittance Spectroscopy*. 2012, Cambridge University Press: Cambridge, United Kingdom. p. 180-220.
42. Nayar, S.K., K. Ikeuchi, and T. Kanade, *Surface reflection: Physical and Geometrical Perspectives.* IEEE Transactions on Pattern Analysis and Machine Intelligence, 1991. **13**(7): p. 611-634.

43. Ahn, J.S., T.R. Hendricks, and I. Lee, *Control of specular and diffuse reflection of light using particle self-assembly at the polymer and metal interface.* Advanced Functional Materials, 2007. **17**: p. 3619-3625.
44. Rengarajan, G., et al., *Albedo measurement system for UVA and the visible wavelength*, in *Radiation Protection Dosimetry: Ultraviolet radiation exposure, measurement and protection*, A.F. McKinlay and M.H. Repacholi, Editors. 2000, Nuclear Technology Publishing: Kent, UK. p. 197-199.
45. Weihs, P., et al., *Measurements of the reflectivity in the ultraviolet and visible wavelength range in a mountainous region*, in *Radiation Protection Dosimetry: Ultraviolet radiation exposure, measurement and protection*, A.F. McKinlay and M.H. Repacholi, Editors. 2000, Nuclear Technology Publishing: Kent, UK. p. 193-195.
46. Frederick, J., H.E. Snell, and E.K. Haywood, *Solar ultraviolet radiation at the earth's surface.* Photochemistry and Photobiology, 1989. **50**(8): p. 443-450.
47. Wang, S.Q., et al., *Ultraviolet A and melanoma: A review.* Journal of American Academy of Dermatology, 2001. **44**(5): p. 837-846.
48. Barker, F., *The Effects of UV-A upon the Eye*, in *Biological Responses to Ultraviolet A Radiation: Second International Conference*, F. Urbach, Editor. 1992, Valdenmar Publishing Company: San Antonio, Texas. p. 273-280.
49. Turner, J., *Ultraviolet radiation reflection: Characterisation, quantification and the resulting effects*, in *Department of Biological and Physical Sciences*. 2011, University of Southern Queensland: Toowoomba, Australia. p. 314.
50. Igoe, D. and A. Parisi, *Evaluation of a smartphone sensor to broadband and narrowband Ultraviolet A radiation.* Instrumentation Science and Technology, 2015. **43**(3): p. 283-289.
51. Igoe, D., *Development and characterisation of a modified smartphone camera for determining UVA aerosol optical depth*, in *Faculty of Health Engineering and Sciences*. 2013, University of Southern Queensland.
52. Igoe, D. and A.V. Parisi, *Broadband direct UVA irradiance measurement for clear skies evaluated using a smartphone.* Radiation Protection Dosimetry, 2015. **167**(4): p. 485-489.